PAPER

Mathematical model for enhancing midwave infrared transmission using phoxonic crystals

Physica Scripta

PAPER

Mathematical model for enhancing midwave infrared transmission using phoxonic crystals

RECEIVED
29 November 2024

ACCEPTED FOR PUBLICATION
17 December 2024

PUBLISHED
30 December 2024

Anurag Sharma[1,2], **Jyoti Kedia**[1] **and Neena Gupta**[1]

[1] Punjab Engineering College (Deemed to be University), Sector-12, Chandigarh-160012, India
[2] Optical Allied and Engineering Pvt. Ltd, Bangalore-560099, India

E-mail: jyotikedia@pec.edu.in

Keywords: mathematical model, phoxonic crystals, waveguide transmission, MWIR

Supplementary material for this article is available online

Abstract

This paper presents a novel mathematical model for designing a highly efficient on-chip optical waveguide operating in the Mid-Wave Infrared (MWIR) spectrum, specifically covering a range from 3–5μm. The proposed waveguide (called Phoxonic waveguide) architecture achieves exceptional transmission rates of up to 99.8% throughout this broad range of MWIR. The simultaneous control of photon and phonon transmission in the proposed waveguide structure gives its name Phoxonic crystal waveguide. The exceptional performance in the proposed waveguide structure has been achieved due to the innovative use of a mirror-symmetric architecture, which effectively suppresses losses caused by the interaction between photons and phonons. To validate the proposed mathematical model's effectiveness, extensive numerical simulations were conducted using the Qutip platform. This research opens promising avenues for the development of MWIR waveguides with wide-ranging applications in communication, defense, medicine, and technology.

1. Introduction

The demand for high-performance mid-wave infrared (MWIR) on-chip sensing solutions is rapidly increasing across various fields, including communication, defense, medicine, and technology [1–5]. Unlike in the shortwave infrared wavelengths where scattering losses are insignificant, the thermal incoherent nature of the source at MWIR and longwave infrared (LWIR) wavelengths makes photon-phonon scattering losses unavoidable and significant. This interaction leads to the loss of photon energy in the form of phonons, which is a major contributor to losses at these higher wavelengths [6].

Recent advancements in nanostructures have led to the proposal of Phoxonic crystals, that exhibit unique properties and offer simultaneous photonic and phononic bandgap [7–11]. These phoxonic crystals enhance the interaction of photons and phonons in the bandgap, effectively retaining high-frequency phonons and reducing the energy loss. Although many researchers have demonstrated enhanced transmission through these structures for near-infrared wavelengths, achieving broad-spectrum waveguides with uniform transmission and low losses remains a challenge [12].

Some unconventional waveguiding approaches, such as suspending the core from the bulk [13–16], have shown considerable reduction in transmission losses. However, these reductions have been limited to a few wavelength peaks with narrow bandwidths. In this research, we propose a mathematical modelling of numerically simulated Phoxonic Crystal Waveguide [17] with a slot structure featuring a new mirror-symmetric architecture that significantly reduces losses due to high-frequency phonon vibrations.

The mirror-symmetric architecture leads to a phenomenon that cancels the momentum of high-frequency phonon vibrations, trap the phonons and prevents their loss in the structure. This novel phenomenon is presented mathematically, demonstrating a significant reduction in the loss of phonon vibrations compared to conventional on-chip optical waveguides such as rib waveguides. This paper presents a mathematical model for designing a highly efficient waveguide operating in the MWIR spectrum, specifically covering the range from 3

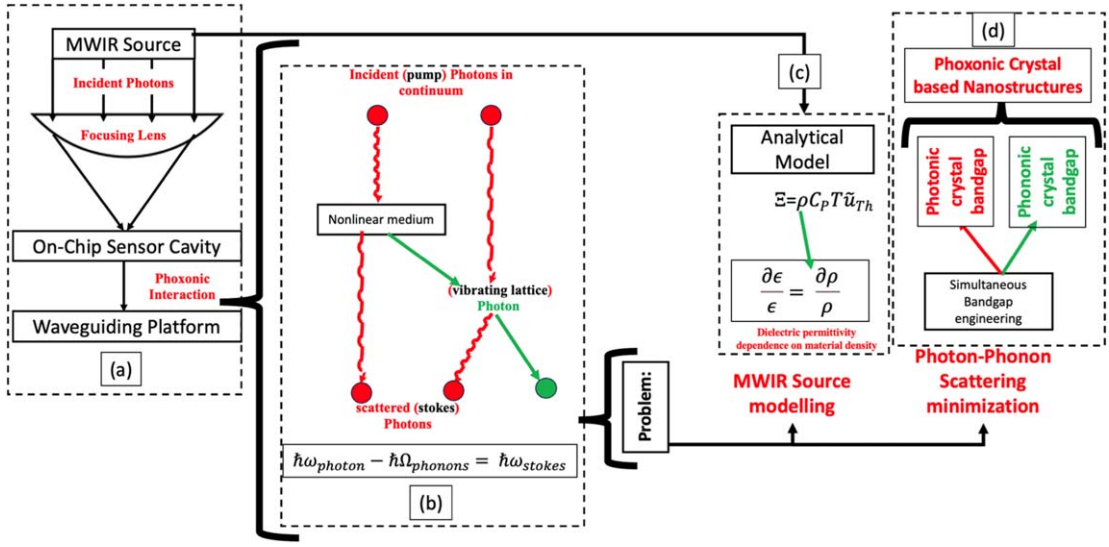

Figure 1. (a) The schematic representation of a typical on-chip sensor cavity fabricated on the waveguide for capturing the thermally-radiating MWIR source which on interacting with cavity membrane tend to generate phonons as a result of lattice vibrations; (b) Illustration of photon-phonon (phoxonic) interaction, causing scattering losses due to unconventional nature of longer wavelength source and nearly comparable Giga-Hertz phonons compared to Tera-Hertz pump photons; (c) the Analytical model for a multispectral MWIR source based on material density dependence over the dielectric permittivity and hence the effective index of the waveguide; (d) Proposed waveguiding solution via tailoring the design parameters for THz-photon confinement and GHz-phonon suppression.

to 5 micrometers. The proposed waveguide architecture achieves exceptional transmission rates of up to 99.8% throughout this broad MWIR range, as validated by extensive numerical simulations using the Qutip [18] and FDTD [19] platform. This research opens up promising avenues for the development of MWIR waveguides with wide-ranging applications in communication, defense, medicine, and technology.

This paper is organized as follows: section 2 describes the theoretical background of Phoxonic Crystal Waveguides and the challenges faced in achieving efficient mid-wave infrared transmission. Section 3 presents the proposed mathematical model for the waveguide design with a novel mirror-symmetric architecture. Section 4 discusses the computational results obtained from the numerical simulations. Section 5 presents a detailed discussion on the suppression of high-frequency translational phonons at the slot boundaries of the proposed Phoxonic Crystal Waveguide with a mirror-symmetric slot structure. This section is followed by section 6, which presents the conclusions drawn from the study and outlines future research directions.

2. Theoretical background

Figure 1(a) illustrates a typical on-chip sensor cavity fabricated on a waveguide for capturing a thermally-radiating MWIR source. The term 'thermally-radiating nature' refers to radiation emitted by objects due to their temperature. In the context of longer wavelength infrared sources, such as those in the mid-wave infrared (MWIR) range, objects naturally emit infrared radiation as a result of their thermal energy or heat.

When incident photons interact with the nonlinear material, the energy of photons reduces and is released in terms of photon-phonon scattering loss as shown in figure 1(b). The fundamental phenomenon that leads to such a scattering loss happens when incident (pump) or captured photons interact in continuum with phonons generated by thermally induced lattice vibrations in the nonlinear medium, see cavity-waveguide interaction. These losses are significant in longer wavelength sources like MWIR, where phonons are nearly comparable in frequency to Tera-Hertz pump photons, leading to unconventional scattering behavior.

Considering the Maxwell equations and the quantum mechanical picture of such an interaction, the relation between magnitude of intensity and phase of photons and phonons becomes critically important to understand. In the linear and isotropic material, the ideal photon-phonon interactions obey the law of conservation of momentum due to phonons of negligible or very small magnitude of intensity. But the magnitude of intensity of phonons becomes large and hence dominant in non-linear materials. These vibrations can be considered as the structural changes in geometry known as moving boundaries effect [20–22], particularly at longer wavelengths. The structural changes may either be longitudinally or translationally vibrating phonons with high-frequency up to few GHz. While the longitudinally vibrating phonons having the same direction as that of incident photons

does not affect the intensity of pump photons, but the translationally vibrating phonons on the other hand counters the pump photons. This causes a phase-mismatch between incoming and scattered photons.

The speed of these pump photons depends on the material's refractive index (n), which is linearly related to its dielectric permittivity (ϵ) of isotropic medium. However, in nonlinear medium, the dependence of dielectric permittivity on the material density (ρ) leads to this unwanted phase-mismatch between pump and scattered photons. This phase-mismatch, which is attributed to change in dielectric permittivity with respect to change in material density at the moving-boundaries, is mathematically represented as:

$$\gamma = \frac{\partial \epsilon}{\epsilon} = \frac{\partial \rho}{\rho} \tag{1}$$

The constant value of gamma (γ) here corresponds to linear and isotropic medium where as $\frac{\partial \epsilon}{\epsilon}\frac{\partial \rho}{\rho}$ signifies the phase-mismatch for the case of anisotropic and nonlinear medium. The time rate of change in phase further corresponds to the frequency of generated phonons. Such a mismatch if suppressed can reduce the intensity of scattered photons against the translationally vibrating phonons.

One of the emerging potential solutions for reducing this scattering loss is the use of the nanostructured materials like topological phoxonic crystals (PxC or optomechanical) as mentioned in figure 1(d). The phoxonic crystals are flexible and offers to tailor the dispersion characteristics of both photons and phonons simply by means of geometry optimization and hence control the change in mode shape to control the phase-mismatch. Given the recent development in waveguide-based sensors using PxCs [23–26], there has been a challenge to achieve uniform optical transmission over a wide range of wavelengths.

In this work, a novel architecture for phoxonic crystals based waveguide architecture has been proposed to offer multispectral optical transmission uniformly over the entire 3–5 μm range. This design aims to effectively confine MWIR photons while minimizing losses caused by phonons. The tailored parameters create bandgaps in the phononic and photonic spectra, ensuring efficient photon transmission while suppressing phonon scattering losses.

3. Proposed waveguide structure

The proposed waveguide is a careful engineering design of a slot waveguide with Phoxonic crystal structure. Phoxonic word is actually a combination of photonic and phononic. In this structure, the sizes of the holes in the crystal structure are varied and strategically placed to achieve the unique properties in the transmission of photons and phonons.

To create a photonic bandgap the uniform sized holes are placed periodically creating change in the refractive index of the material However when we Place periodically the different sized holes, it creates a phononic bandgap since the uniform pattern of different sized holes create a change in the material density. This bandgap for phonons prevents certain phonon modes from propagation. Hence the phonons are trapped within the crystal lattice. This simultaneous creation of photonic and phononic band gap give rise to unique property of this structure that when photons strike the crystal lattice and create phonons, these phonons are trapped within the wave guide and hence, do not lose their energy in the crystal lattice.

Further, it has been observed that the phonons which are travelling in the same direction as that of photons do not cause scattering. However, the phonons which are travelling in the transverse direction cause major scattering of the photon particles. In the proposed structure as shown in figure 2, The placement of the phoxonic crystal unit cell is such that it creates a kind of mirror symmetry around the slot wave guide. This mirror symmetry causes equal and opposite momentum of the generated phonons leading to neutralisation of the scattering of photons by these phonons. This leads to the reduction of scattering of photons significantly enhancing transmission efficiency. The choice of the parameters such as slot width, slot height, whole radius lattice periodicity and the number of air holes in each row requires extensive simulations and optimization techniques It is very critical to decide these parameters for ensuring the optimum performance of the waveguide That is highly efficient photon transmission with minimum scattering due to phonons.

These optimized parameters for the proposed waveguide are: the slot width (w = 622.4489 nm), slot height (h = 561.2249 nm), radius of the large air hole (R = 312.2449 nm), radius of the small air hole (r = 156.1224 nm), lattice periodicity (a = 1608.1633 nm), and number of air holes in each row (n = 2).

Figure 2(a) illustrates the design of a 2D Ge/SiGe slot-waveguide structure by periodically repeating the entire unit cell in the propagation direction (y) with an optimized lattice periodicity (a) to ensure uniform transmission across the entire spectrum. Figure 2(b) illustrates a single unit of the slot-waveguide architecture, featuring the slot (w = 622.4489 nm, h = 561.2249 nm), large air hole (R = 312.2449 nm), small air hole (r = 156.1224 nm), and lattice periodicity (a = 1608.1633 nm), with two air holes in each row. Figure 2(c) illustrates the waveguide structure, formed by periodically repeating the two mirror-symmetric phoxonic crystal

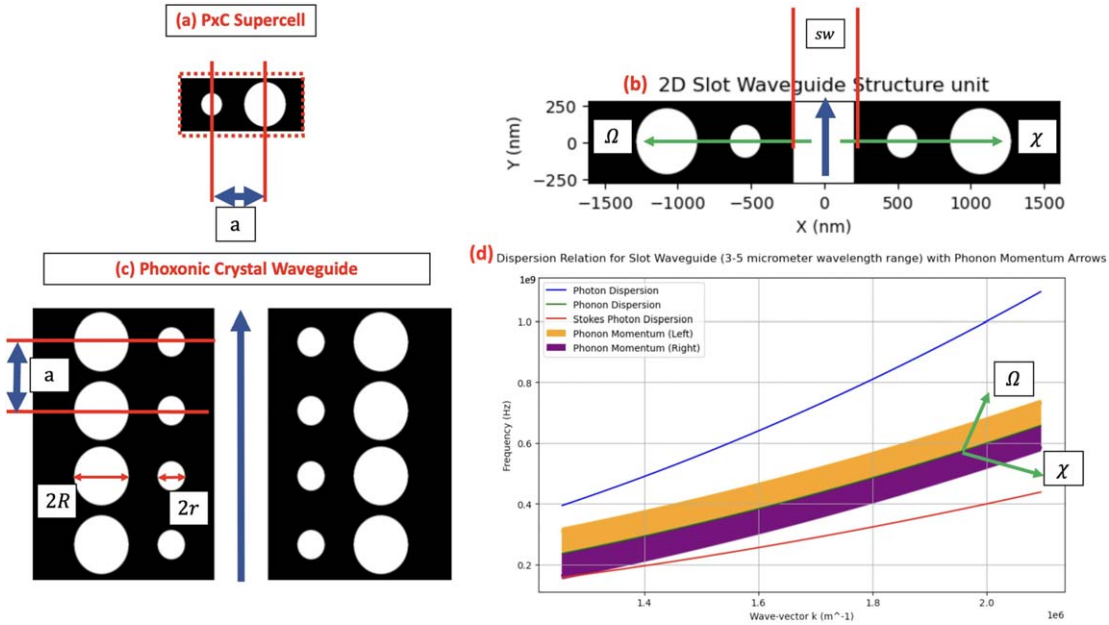

Figure 2. (a) Design of a single phoxonic crystal (PxC) supercell formed using small and large oxide holes in a SiGe membrane. (b): Design of a 2D slot waveguide unit formed by mirror-symmetric placement of two PxC supercells. (c): The numerically simulated 2D Ge/SiGe PxC-based slot-waveguide structure by periodically repeating the entire mirror-symmetric unit-cell in the propagation direction (y) with an optimized lattice periodicity, a to ensure uniform transmission across the entire spectrum, the green arrows represents the transversely travelling flexural phonons of the two mirror-symmetric PxC supercells exhibiting equal and opposite momentum (illustrated as derived phonon frequency: Ω and χ; (d): The plot between frequency and wave-vector (k) is used to analyze the dispersion relation, which relates the frequency of a phonon mode to its wave-vector. The equal and opposite momentum of translational phonons (marked as orange and purple shades) in mirror-symmetric PxC supercells is evident, leading to a cancellation effect and enhanced transmission efficiency in the PxC-slot waveguide.

(PxC) supercells along the *y*-axis (propagation direction), showcasing its design optimized to suppress Stokes (or scattered) photon dispersion caused by translationally vibrating phonons (high-frequency). In figure 2(d), The plot between frequency and wave-vector (k) is used to analyze the dispersion relation, which relates the frequency of a phonon mode to its wave-vector. The wave-vector is related to the waveguide geometry parameters such as lattice periodicity and the size of the unit cell. The equal and opposite momentum of the translational phonons in the two mirror-symmetric phoxonic crystal (PxC) supercells is evident through the spatial arrangement of the structure. The symmetrical placement of the supercells leads to a cancellation effect, where the phonon momentum transfer from one supercell counteracts the momentum transfer from the other.

In the context of the PxC-slot waveguide, the reduction in phonon displacement signifies a cancellation of momentum, which is represented by the reduction in the slope of the dispersion curve. This cancellation effect leads to the suppression of phonons, resulting in enhanced transmission efficiency. Structurally, this symmetrical arrangement alters the momentum transfer within the waveguide, enhancing the transmission of pump photons through the slot region. The relationship between the structure and this cancellation effect is crucial, as it allows for the efficient transmission of photons with minimal phonon interference, improving the overall performance of the waveguide. The marked phonon frequencies Ω and χ, corresponding to the two mirror-symmetric supercells, are derived mathematically in a later section. This cancellation results in a reduction of the impact of phonons on the transmitted photons.

Figures 2(a)–(d) visually represent the exceptional performance of the waveguide structure.

To bridge the discussion on the proposed waveguide structure with the mathematical model and analysis, it is essential to highlight the need for conservation of energy and momentum of photons in the waveguide design. Conservation of energy and momentum is crucial for maintaining the integrity of the optical signal within the waveguide structure. When photons interact with the waveguide material, they can scatter or be absorbed, leading to signal loss. To minimize these losses and ensure efficient transmission, it is essential to match the phases of the incoming and outgoing photons. The phase matching of pump and Stokes photons involves synchronizing their oscillations so that they reinforce each other rather than cancel out. This synchronization is achieved by designing the mirror-symmetric slot-waveguide structure which ensures the suppression of scattered photons (stokes) due to controlled interactions between pump photons and the material's lattice vibrations (phonons). This anticipates the enhancement in the effective optical transmission through the slot waveguide.

Conclusively, the efficient transmission relies on matching the phases of incoming and outgoing photons which is being achieved by manipulating photon-phonon interactions. This synchronization ensures that the energy and momentum of photons are conserved throughout the waveguide structure. The base Hamiltonian is evolved over space and time to determine the complex frequency of the target phonons, as shown in the photon-phonon dispersion relation in figure 2. The term 'base Hamiltonian' refers to the fundamental mathematical framework used to describe the interactions between photons and phonons in the waveguide. By evolving this Hamiltonian, researchers can calculate the frequencies at which phonons are generated or absorbed, allowing them to design the waveguide in a way that suppresses these phonons. This understanding forms the basis for developing the mathematical model and conducting the analysis presented in the subsequent sections.

4. Mathematical model and analysis

To develop the mathematical model for the waveguide architecture, we start with the conventional model for on-chip optomechanical effects computation [10, 27]. This model needs to account for both thermal radiation pressure and traditional phonon field variations, especially at longer wavelengths. It is essential to represent the modified phonon-field variation resulting from the incident photonic field or electromagnetic wave propagating in the y-direction. This representation is crucial for understanding the interaction between photons and phonons in the waveguide structure. The model considers the waveguide architecture featuring a Germanium (Ge)-slot waveguide surrounded by an array of oxide holes within a Silicon-Germanium (SiGe) membrane.

In the context of waveguide design, conserving the energy and momentum of photons is crucial for maintaining the integrity of the optical signal [10]. When photons interact with the waveguide material, they can scatter or be absorbed, leading to signal loss. To minimize these losses and ensure efficient transmission, it is essential to match the phases of the incoming and outgoing photons. Matching the phases of pump and Stokes photons involves synchronizing their oscillations so that they reinforce each other rather than cancel out. This synchronization is achieved by designing the waveguide structure to manipulate the interactions between photons and the material's lattice vibrations (phonons). The idea used in this work was carefully controlling these interactions, by means of which designers can ensure that the energy and momentum of the photons are conserved (see photon-phonon dispersion relation shown in figure 2). This is achieved by evolving the base Hamiltonian over space and time to determine the complex frequency of the target phonons. In this specific case, the waveguide structure employs a mirror-symmetric geometry, as shown in figure 2, which plays a crucial role in suppressing the target phonons. This approach not only helps in reducing losses but also enhances the overall efficiency of the waveguide in guiding MWIR photons.

Therefore, starting with the conventional model [10], in this work, the modified phonon-field variation resulting from the incident photonic field or electromagnetic wave propagating in the y-direction is represented as spirally-displaced boundaries. This spiralling variation in material density, as shown in figure 3, is crucial for understanding the interaction between photons and phonons in the waveguide structure. As phonons travel through the waveguide, they cause the boundaries to oscillate or deform, while translationally interacting with the waveguide boundaries. This leads to spiral-like (flexural) pattern generation on the boundaries. This variation in the edges of the waveguide due to translationally travelling flexural phonon modes is known as Moving Boundary Effect (MBE). The translationally vibrating phonons refer to phonon modes in which atoms or molecules within a lattice move linearly in a coordinated, back-and-forth motion along a specific axis. Unlike rotational or flexural phonon modes, where the motion involves angular displacement or bending, translational phonon modes involve straight-line, oscillatory motion of atoms relative to their equilibrium positions. This type of vibration is critical in determining the interaction between phonons and photons, especially in the mid-infrared (MWIR) range, where translational phonon activity can influence energy dissipation and optical transmission efficiency. In the context of our proposed waveguide structure, controlling these translational phonon modes helps to minimize phonon-related losses, thereby improving overall transmission performance. Such translational phonon modes can impact the overall energy dynamics of the waveguide, contributing to heat dissipation or interaction with photons in a way that influences optical transmission. That is why these modes are required to be tailored when considering phonon-related losses in waveguides, especially at the mid-infrared (MWIR) range where phonon activity can affect material properties. In figure 3, the spiral-like variation in the Rib waveguide's displacement due to translational phonon modes is linked to the Moving Boundary Effect (MBE). In contrast, the PxC-slot waveguide shows reduced phonon displacement, indicating less deformation of the waveguide boundaries. This reduction in phonon-induced boundary movement demonstrates the effectiveness of the PxC-slot waveguide in suppressing the Moving Boundary Effect (MBE). By minimizing the MBE, the PxC-slot waveguide can maintain a more stable waveguiding structure, resulting in improved transmission efficiency (figure 3(e)) and reduced losses compared to conventional Rib waveguides over desired the MWIR spectrum. The reduced displacement in the PxC waveguide compared to the rib waveguide

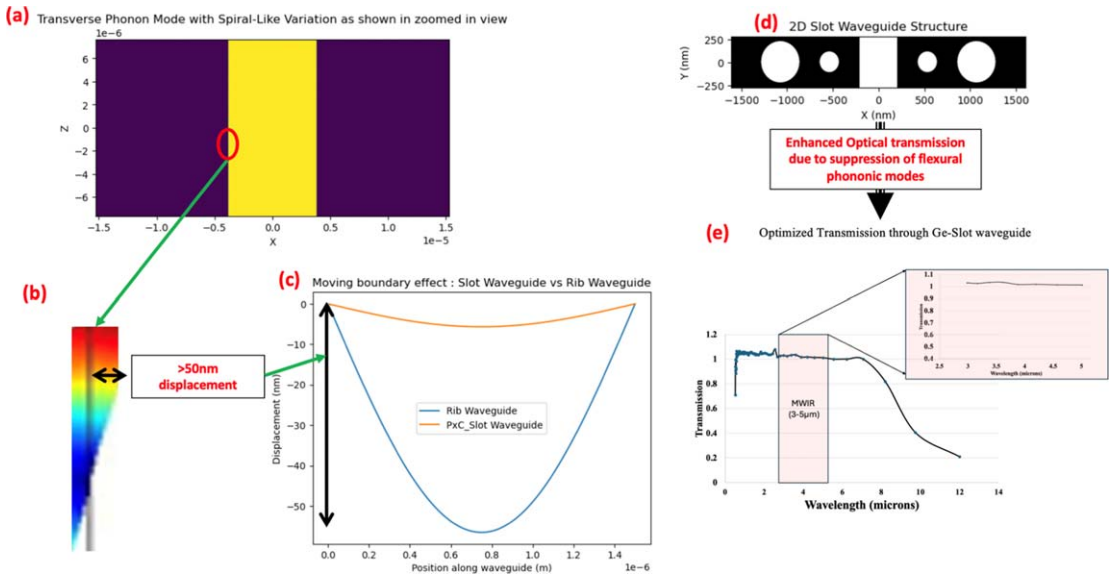

Figure 3. (a) Numerically simulated spiral-like variation due to the transverse phonon mode in a conventional Rib waveguide, also shown in (b). zoomed in view and (c). the linear graph between transverse phonon displacement versus position along waveguiding axis in comparison with (d). proposed PxC-slot waveguide. The reduction in phonon displacement in the proposed slot-waveguide results in (e). the enhanced optical transmission due to the suppression of flexural phonon modes.

demonstrates the effectiveness of the PxC waveguide in suppressing this effect, leading to improved transmission efficiency and reduced losses.

The representation of this variation is expressed in the following equations [21]:

$$\tilde{u}(y) = \sum_{k} (\tilde{u}_k + \widetilde{u}_{Th})[\hat{b}_k e^{iky} + H.c] \tag{2.a}$$

$$\widetilde{E_{th}}(y) = \sum_{k} \tilde{E}_k[\hat{a}_k e^{iky} + H.c] \tag{2.b}$$

The $\tilde{u}(y)$ represents the modified phonon field while $\widetilde{u}_{Th}$ is the thermally-varied phonon displacement field, $\widetilde{E_{th}}(y)$ is the electric field component of the thermally-varied electromagnetic wave, $\tilde{u}_k$ and $\tilde{E}_k$ are the field components of phonons and photons, respectively, and $\hat{a}_k$ and $\hat{b}_k$ are the annihilation operators for photons and phonons, respectively. These equations form the basis of our mathematical model for analysing the interaction between photons and phonons in the waveguide structure.

Referring to the Dirac notation, $\hat{a}_k$ and $\hat{b}_k$ are the photon and phonon annihilation operators, respectively, with 'k' representing the wave-vector defining the space-domain. The number of annihilated (slowed down or suppressed) phonons can be measured by multiplying the operator with its complex conjugate, known as the phonon number ($\hat{b}_k{}^{\dagger}\hat{b}_k$) Similarly, the count for the number of traveling photons through the waveguide is defined by the photon number ($\hat{a}_k{}^{\dagger}\hat{a}_k$). Given the longer wavelengths like MWIR, to account for the thermal behavior of the phoxonic (photon-phonon) interaction at waveguide boundaries, the discrete heat-convection [27] along with moving-boundary conditions were assumed. Following this, the k-mode field component of the thermally-varied phonon displacement field, $\widetilde{u}_{Th}$, is analytically modelled (see supplementary data) in terms of the heat flux (Ξ) and thermal temperature ($\lambda T = 0.2898$ cm Kelvin) with C_P being the specific heat of the material.

$$\widetilde{u}_{Th} = \left(\frac{\Xi}{\rho C_P T}\right) \tag{3}$$

The quantum optomechanical model by M. Tomes [11] provides a basis for developing an equivalent model for the phoxonic interaction in the waveguide. The base Hamiltonian for this interaction is given by:

$$\hat{\mathcal{H}} = \int_0^{t_s} dz \left[\frac{\hat{\Pi}^2(y)}{2A_s\rho} + \frac{A_s P}{2}((\partial_y \tilde{u}_k))^2 + \frac{A_{OPT}\,\gamma\,(\partial_y \tilde{u}_k){E_{th}}^2}{2} + \cdots\cdots \text{Supplementary data}\right] \tag{A.1}$$

where;

- with $\hat{\Pi}^2(y) = A_s\rho$ represents the momentum density function across the moving boundaries.

- A_s is the phoxonic interaction area with a thickness of t_s and slot-width 'sw', taken as twice that of the optical mode area A_{OPT} [12].
- The term $\left(\frac{1}{2} A_s \mathrm{P} (\partial_y U) E^2\right)$ represents the contributing phonon field due to elastic phonon displacement U, where P is the equivalent spring constant per unit area.
- The momentum transfer due to the total phonon field can be formulated from the kinetic energy relation: $\frac{\hat{\Pi}^2(y)}{P} = \left(\frac{1}{2} A_s \rho \dot{U}^2\right)$.
- The additional term $\left(\frac{1}{2} A_{OPT} \gamma (\partial_y U) E_{th}{}^2\right)$ is added to model the varying phonon displacement in the direction of propagation resulting from the photo-thermal field, E_{th}
- γ is the phase-mismatch due to material nonlinearity as shown in equation (1), and A_{OPT} is the area of the photon (or optical) frequency mode.
- It is assumed that the thermally-radiating MWIR photon field is uniformly distributed across the whole sensing cross-section. Given the law of heat convection for the discrete boundaries of the slot waveguide, the k-space component of the phonon displacement field $\tilde{u}_k$ ('Th' representing thermally-varying) as described in equation (2.a) above.

The slot width is chosen to be twice that of the optical mode area A_{OPT} to maximize the confinement of the optical mode, a common practice in conventional slot waveguides. This choice is based on the fact that the cross-section area of the mechanical phonon field (A_m) is much smaller than that of the optical photon field cross-section area [28]. This design principle aims to enhance the interaction between photons and phonons while minimizing losses, ultimately contributing to the overall effectiveness of the waveguide configuration.

The rationale behind selecting a slot width twice that of the optical mode area lies in achieving optimal optical mode confinement. In slot waveguides, this approach helps to ensure that a significant portion of the optical mode is localized within the slot region, where the interaction with the mechanical phonon field primarily occurs. The larger slot width allows for better overlap between the optical and phononic fields, enhancing the efficiency of photon-phonon interactions. Furthermore, by maximizing the confinement of the optical mode, the waveguide can effectively manipulate the phase matching conditions required for efficient photon-phonon interactions. The base Hamiltonian, describing the interactions between photons and phonons, is evolved over space and time to derive the complex frequency of the translational phonons. This complex frequency, denoted as Ω_k, is a crucial parameter that influences the behavior of the phonons and their interaction with photons in the waveguide, derived as follows (see supplementary data).

$$\Omega_k = \rho\left(\frac{\xi C_P T}{\Xi}\right)^2\Bigg]_k = |\mathrm{k}|\, v_{pn} \tag{4}$$

The phonon frequency is typically a function of the phase velocity v_{pn}, which represents its displacement in k-vector space. In our model, the direct dependence on the material density function and the thermally-radiating field simplifies the relationship between the photon and phonon fields, especially at longer wavelengths. After deriving the density-dependent phonon frequency, an additional term, $\hat{\mathcal{H}}_{inter}$, is introduced to represent the phoxonic interaction within the quantum nonlinear optics regime for phoxonic nanoscale waveguides [29, 30].

$$\hat{\mathcal{H}}_{inter} = \begin{pmatrix} Gain1 & \mathrm{g}(+) \\ \mathrm{g}(+) & Loss1 \end{pmatrix} + \begin{pmatrix} gain2 & \mathrm{g}(-) \\ \mathrm{g}(-) & loss2 \end{pmatrix} \tag{5}$$

This shows how the photon and phonon fields are being interacted within the given slot waveguide boundaries. The coherently interacting photons and longitudinal phonons will be contributing forward or backward photonic modes, represented as diagonal Gain or Loss terms, respectively. The phoxonic interaction between pump photons and longitudinal phonons propagating along the same direction constitutes the Gain term, while the interaction with counter-propagating longitudinal phonons constitutes the Loss term.

- The off-diagonal terms denoted by nonlinear gain term 'g(±)' is used to represent the effect of translationally-vibrating transverse phonons explained in figure 3 with the forward photonic mode. These are the incoherent energy terms resulting from thermally-varying density function.
- The sign '+' signifies the photon-phonon scattering effect constituting losses due to interaction between pump photon through the slot region and the k-space unit-cell with smaller radius, r as the exponential

argument ($\exp^{j(r\phi_j+y_j)}$) periodically repeating boundary condition in propagation direction of pump photons modelled as $\hat{\mathcal{H}}_{inter1}$.

- The '-' sign refers to the photon-phonon scattering effect constituting losses which could propagate along the slot-region boundaries. The $\hat{\mathcal{H}}_{inter2}$ is thus modelled as a function of g(−) with scattering loss being terminated by the unit-cell with larger radius, R described by the exponential argument $\exp^{j(R\phi_j + x_j + y_j)}$ which shows periodically repeating boundary condition in propagation direction of pump photons ('y') as well as the translational phonon momentum in 'x' direction.
- The subscript 'j' accounts for periodically repeating holes in k-space equivalent. The two interaction terms are represented as follows with Hermitian conjugates (h. c) ,

$$\hat{\mathcal{H}}_{inter1} = g(+)\left[\sum_{j=k} \sigma_j{}^{\dagger} c_j \exp^{j(r\phi_j + y_j)}\right] + h.c \tag{6.a}$$

$$\hat{\mathcal{H}}_{inter2} = g(-)\left[\sum_{j=k} (a_j{}^{\dagger}\, a_j) c_k \exp^{j(R\phi_j + y_j + x_j)}\right] + h.c \tag{6.b}$$

Increasing the value of j would involve repeating the pattern of the photonic crystal array of holes, which can enhance the reflectivity of the optical cavity formed between the slot-waveguide boundaries. This enhancement occurs because the repeated pattern creates more opportunities for light to be reflected back into the cavity, increasing the chances of guiding the pump photons effectively [31]. However, this enhancement comes at a cost, specifically in terms of simulation time. Increasing the value of j means simulating a larger and more complex structure, which requires more computational resources and time to accurately model the behavior of light within the cavity. This trade-off between reflectivity enhancement and increased simulation time needs to be carefully considered based on the specific requirements and constraints of this research.

Hence, a single layer periodically repeating in the direction of propagation of incident photons through the waveguide slot-region was considered. The cavity with a quality factor (Q) was then taken into account [32], and the Hamiltonian was evolved over the phonon lifetime (~ps) and in k-space over the propagation length of the waveguide, L, thereby expressing the nonlinear gain term as:

$$g(\pm)^2 \approx \upsilon_{pn}{}^2 \frac{\hbar^2}{2m} \Theta_{NL}(E_{th}\,(\Omega \pm \chi)/(L_m Q_m)) \tag{7}$$

Here, $g(\pm)$ represents the nonlinear gain term, υ_{pn} is the phonon velocity in the medium, and Θ_{NL} is the intrinsic gain due to material nonlinearity [28]. Equation (7) depicts $g(+)$ and $g(-)$ as two possibilities, one showing the addition of the phonon frequency $(\Omega + \chi)$ while the other being the subtraction $(\Omega - \chi)$ respectively. In the slot region, it is necessary to enhance the nonlinear gain $g(+)$ in the direction of propagation (forward photonic mode) and suppress the nonlinear gain $g(-)$ in the opposite and translational direction (backward photonic mode). By utilizing mirror symmetry to achieve opposite and equal phonon momentum, as depicted in the dispersion relation, it is possible to satisfy the phase-match conditions required to diminish the latter term by maintaining $\Omega = \chi$ and suppressing the backward gain term.

The idea presented in the previous paragraph form the basis for understanding the nonlinear gain mechanisms crucial to the proposed phoxonic crystal (PxC) waveguide's functionality. To delve deeper, it then turns to a quantum optical perspective to elucidate the behavior of mass density as a function of the incident photon wave-function [33]. With reference to the quantum optical picture for the case of chiral waveguide systems, where the mass density represented as a function of the incident photon wave-function ψ can be denoted as $\rho = |\psi\rangle\langle\psi|$.

The time-evolution of the system from its pure state ($\psi|$) was varied over a finite range of temperature and hence representing the final thermally perturbed material density matrix as a classical probability function: p_i directly proportional to canonical partition function: $Z = \sum_i \exp^{[-\beta E_i]}$, given $E_i = \widetilde{E_{th}}(z)$. In the quantum optical picture, the mass density ρ s represented as a function of the incident photon wave-function ψ. The time evolution of the system from its pure state $\psi|$ was varied over a finite range of temperature, representing the final thermally perturbed material density matrix as a classical probability function p_i directly proportional to canonical partition function: $Z = \sum_i \exp^{[-\beta E_i]}$, given $E_i = \widetilde{E_{th}}(z)$.

$$\rho = \sum_i \rho_i |\psi_i\, \psi_i| = \sum_i \exp^{[-\beta E_i]} |\psi_i\, \psi_i| = \exp^{[-\beta \hat{\mathcal{H}}_{inter}]} \tag{8}$$

This equation describes the time evolution of the system's density matrix ρ under the influence of an interaction Hamiltonian $\hat{\mathcal{H}}_{inter}$ at a finite temperature. Here, a set of incident $\mathbb{N}$-particles in linear material-dimensions: $\mathcal{R} = \{r_1, r_2, \ldots, r_{\mathbb{N}}\}$ interacts in the nonlinear material-dimensions $\{\mathcal{R}'\}$. The thermal density matrix is then

reformulated over the photon-phonon interaction Hamiltonian in z-direction generating translational phonons and hence scattered photons.

$$\rho\ (\mathcal{R},\ \mathcal{R}';\ \beta) = \sum_i \rho_i \mathcal{R}|\exp^{[-\beta\mathcal{H}]}|\mathcal{R}' = \sum_i \exp^{[-\beta\mathcal{H}]}\ \psi_i^*(\mathcal{R})\psi_i(\mathcal{R}') \tag{9}$$

Ideally, any conventional Hermitian or linear systems perturbed by nonlinear ambience must satisfy the condition: $\rho\ (\mathcal{R},\ \mathcal{R}';\ \beta) \neq \rho\ (\mathcal{R}',\ \mathcal{R};\ \beta)$ [34]. Upon solving the expectation values along the moving slot boundaries while knowing the stochastic and asymmetric nature of phoXonic interactions, we get:

$$\wp = \frac{1}{Z_1}\left[\int d\mathcal{R}\ \rho(\mathcal{R},\ \mathcal{R}';\ \beta')\mathcal{R}|\wp|\ \mathcal{R}'\right] + \frac{1}{Z_2}\left[\int d\mathcal{R}'\rho(\mathcal{R}',\ \mathcal{R};\ q)\mathcal{R}'|\wp|\mathcal{R}\right] \tag{10}$$

The propagation constant (β) of the incident (or pump) photons, after the phoXonic interaction splits to scattered photons (β') and phonons (q). For simplicity, the Plane-wave Eigenmode 1D solution, with source wave function ($\psi_N(r) \cong \frac{1}{V}\ e^{-k_n \cdot r}$); for a free particle in a periodically repeated box of size, L_m and waveguide volume, $\mathrm{V} = {L_m}^D$, $k_n = \frac{2\pi n}{L_m}$) is solved. The slot region of the waveguide which was assumed as an equivalent of a resonating cavity discussed previously. Thus, the two supercells acting as reflecting mirrors with, $\mathrm{Wq} \ll {L_m}^2$; where $\mathrm{W} = \frac{\hbar^2}{2m}$ and $L_m\ (= v_a \tau_{TRT})$ are modelled for trapping the suppressed thermal phonons with phonon velocity (v_a) and thermal relaxation-time (τ_{TRT}). The thermal relaxation time is typically assumed to be equal to non-radiative decay rate (Γ). The final thermal density matrix for the given problem representing translational phonons is derived as:

$$\begin{aligned}\rho(\mathcal{R}',\ \mathcal{R};\ q) &= \sum_n \frac{1}{V}\ e^{-q\lambda \mathrm{T}^2 + ik_n(r-r')} \\ &= (4\pi \mathrm{T}q)^{-\frac{D}{2}} \sum_n e^{\left(-\frac{(r-r'-nL_m)^2}{4\mathrm{T}q}\right)} \\ &\approx (4\pi \mathrm{T}q)^{-3/2} \sum_n e^{\left(-\frac{(r-r')^2}{4\mathrm{T}q}\right)}\end{aligned} \tag{11}$$

Given the non-Hermitian eigen-value problem [35], the parity-time symmetry in space and time can be used, which results in converting the non-Hermitian to Hermitian dynamics at symmetric points so as to obtain the real eigenvalues signifying lossy terms. And hence the final validation of the following relation, which proves that despite the existence of translational phonons the lossy g(-) term distinguishes due to mirror-symmetric PxC supercells.

$$\rho\ (\mathcal{R},\ \mathcal{R}';\ q) = \sum_n \frac{1}{V}\ e^{-q\lambda \mathrm{T}^2 + (-i)k_n(r'-r)} = \rho\ (\mathcal{R}',\ \mathcal{R};\ q) \tag{12}$$

After deriving equation (12) to represent the thermal density matrix for translational phonons, the behavior of this thermal density relation in the proposed non-Hermitian system is demonstrated. This relation, resembling what is expected in a Hermitian system, confirms a crucial symmetry property for the analysis. This symmetry simplifies the dynamics of the system, providing a clearer understanding of how photons and phonons interact within the waveguide. These findings set the stage for the experimental validation discussed in the results section, where the practical implications of the model in guiding the design of advanced photonic devices are explored.

5. Results

To validate the analytical model, simulations were conducted using the Qutip library, a Python-based open-source platform for quantum computing and quantum information processing. The simulations involved the time evolution of the Hamiltonian, which describes the dynamics of the system under consideration. The simulations aimed to calculate the interaction between photons and phonons within the waveguide structure. This interaction is crucial for understanding the behavior of the system, especially in terms of how the photonic and phononic fields coherently interact and contribute to the overall transmission properties of the waveguide.

To simulate this interaction, we first defined the Hamiltonian that represents the phoxonic interaction within the waveguide. This Hamiltonian includes terms that account for the gain and loss processes, as well as the coherent and incoherent interactions between photons and phonons. The time evolution of this Hamiltonian was then calculated using Qutip, which allowed us to study how the system evolves over time and how the different parameters affect its behavior. Overall, the simulations were conducted to validate the proposed analytical model and to gain insights into the underlying physics of the waveguide structure. The results of these simulations were used to refine the model and to ensure its accuracy in predicting the

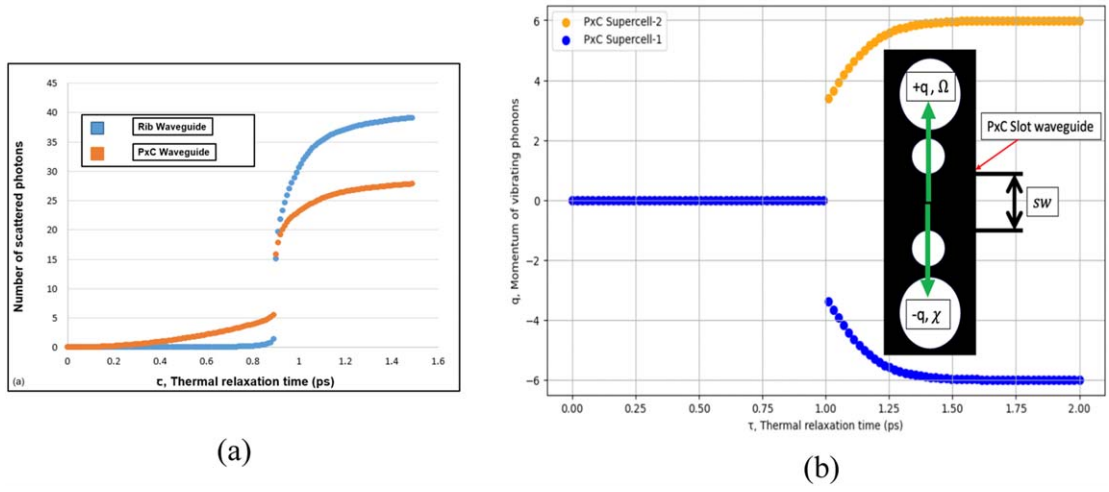

Figure 4. (a) The relation between number of vibrating atoms (scattered photons) versus thermal relaxation time for simple rib and PxC waveguide, and (b) the momentum transferred to the translational phonons (green arrows) versus the thermal relaxation time for mirror-symmetric PxC supercells.

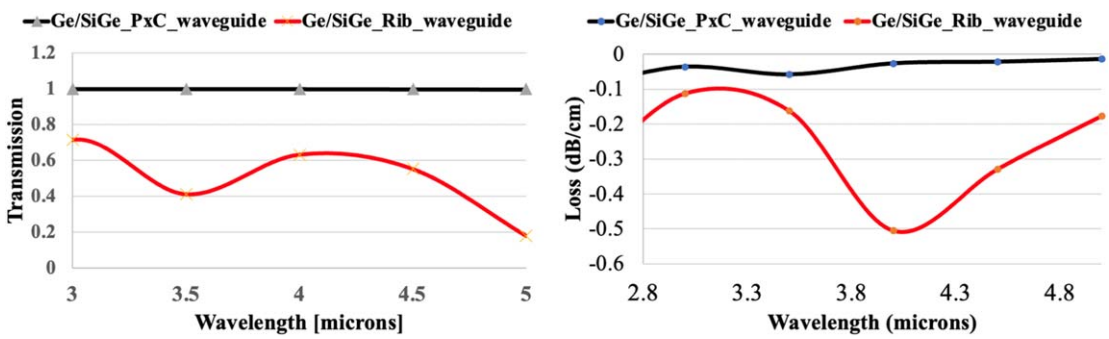

Figure 5. The transmission characteristics of Ge/SiGe waveguide, one with proposed PxC-based architecture (red) compared with simple Rib waveguide architecture (black) [24].

transmission properties of the waveguide. Figure 4(a) compares the scattered photons due to translational phonons in both the simple rib waveguide and the proposed PxC waveguide, plotted against the thermal relaxation time of phonons. This comparison is crucial for validating the effectiveness of the proposed PxC waveguide design in suppressing photon-phonon interactions, especially at shorter thermal relaxation times.

The thermal relaxation time represents the timescale over which the thermal energy in the system dissipates, affecting the interactions between photons and phonons. At shorter thermal relaxation times, the thermal energy dissipates quickly, leading to more pronounced interactions between photons and phonons. The graph clearly shows that the PxC waveguide exhibits significantly lower scattered photons compared to the simple rib waveguide, especially at shorter thermal relaxation times. This suppression of scattered photons in the PxC waveguide is a result of the precisely engineered opposite angular momentum of the translational phonon contributions from the two supercells, as further illustrated in figure 4(b).

Figure 5 illustrates the transmission characteristics of the Ge/SiGe waveguide, comparing the proposed PxC-based architecture (red) with a simple Rib waveguide architecture (black). The transmission is plotted against the wavelength of the incident photons, ranging from 3 μm to 5 μm. The graph clearly shows that the PxC-based architecture outperforms the simple Rib waveguide, achieving higher and more uniform transmission over the entire spectrum. This improvement is attributed to the unique properties of the PxC structure, which effectively suppresses photon-phonon interactions and minimizes losses, leading to enhanced transmission efficiency. The superior performance of the PxC-based architecture makes it a promising candidate for midwave infrared (MWIR) transmission applications, where high transmission efficiency and uniformity are essential. Furthermore, the PxC design offers flexibility in tuning the transmission characteristics by adjusting the geometrical parameters, making it a versatile platform for on-chip photonic applications.

Table 1. The comparison of proposed PxC slot-waveguide with recent literature.

References	Technology	Waveguide architecture	Waveguide core		Peak wavelength (μm)	Bandwidth (μm)	Transmission loss (dB/cm)
			Width (μm)	Height (μm)			
2018 [20]	Graded SiGe on SOI	Rib	1.182	0.865	6.4	5.4–8.4	2–3
2020 [14]	Graded SiGe on SOI	Rib	1.584	0.487	8.5	7.5–9.4	2–20
2021 [19]	Si on SOI	Suspended Rib	0.09874	0.1915	4	3.7–4.1	2–9
2022 [21]	InGaAs/InP	Ridge	0.98	1.08	5.35	5–11	0.5–4.5
2023 [17]*	Graded SiGe PxC on SOI	Slot	1.16	1.29	Uniform throughout	3–5	<0.1

6. Discussion

The successful design and optimization of a Ge/SiGe slot waveguide for Terahertz photonic applications, achieving uniform transmission over the entire test range of 3–5 μm, mark significant progress. With a transmission loss ranging from 0.1–0.25 dB/cm, the optimized waveguide structure outperforms other technologies, such as graded SiGe on SOI rib waveguides. A comparison with recent literature (table 1) highlights the superior performance of the proposed Ge/SiGe slot waveguide. Notably, the proposed waveguide offers lower transmission loss and a wider bandwidth, positioning it as a promising candidate for Terahertz photonic applications.

In the context of recent advancements in waveguide technologies, the performance of the proposed Ge/SiGe slot waveguide stands out. The 2018 [20] study by Eggleton *et al* on graded SiGe on SOI rib waveguides achieved a transmission loss of 2–3 dB/cm over a bandwidth of 5.4–8.4 μm. Similarly, the 2020 [14] work by Liu *et al* focused on graded SiGe on SOI rib waveguides, reporting a transmission loss of 2–20 dB/cm and a bandwidth of 7.5–9.4 μm. Contrastingly, the 2021 [19] study by Daniel Ho *et al* explored Si on SOI suspended rib waveguides, achieving a transmission loss of 2–9 dB/cm over a bandwidth of 3.7–4.1 μm. In comparison, the proposed Ge/SiGe slot waveguide in this study demonstrates superior performance with a transmission loss of 0.1–0.25 dB/cm and a uniform transmission throughout the 3–5 μm range. Moreover, the proposed waveguide's bandwidth and transmission loss outperform the InGaAs/InP ridge waveguides discussed by Wiederhecker G *et al* in 2022 [21], which reported a transmission loss of 0.5–4.5 dB/cm and a bandwidth of 5–11 μm.

In validating the assumptions of the presented mathematical model, extensive numerical simulations were conducted to ensure that the model accurately represents photon-phonon interactions within the structure of photonic crystals. This involved comparing the simulation results with existing theoretical predictions and experimental data found in the literature, confirming that the model reliably captures the underlying physics governing these interactions. The Qutip platform was chosen for our numerical simulations due to its robustness in handling quantum mechanical interactions for non-Hermitian systems and its efficiency in solving the underlying equations governing photon and phonon dynamics. Additionally, the results of Qutip were then used as a basis for Finite-Difference Time-Domain (FDTD) based waveguide simulations. Regarding the high transmission rates observed in the 3 to 5 μm range, extending this range to other wavelengths, such as the far infrared, could enhance the waveguide's applicability in a wider array of technologies. This extension would allow for potential use in sensing applications, particularly in areas like environmental monitoring and chemical analysis, where far-infrared spectroscopy is crucial for detecting specific molecular signatures. The selection of the 3 μm to 5 μm wavelength range is crucial for Mid-Wave Infrared (MWIR) applications, as it encompasses key spectral features important for environmental monitoring, gas sensing, and thermal imaging. This range includes molecular absorption lines for gases such as CO_2, CH_4, and H_2O, making it highly relevant for detecting and monitoring these substances. Additionally, the optical materials used in the Phoxonic crystal waveguide exhibit favourable transmission properties within this range, ensuring efficient light propagation and minimal losses. While computational constraints required a focused approach on this range, the insights gained from these simulations are expected to apply to longer infrared wavelengths, expanding the potential applications of the waveguide to fields such as telecommunications and medical diagnostics, where low-loss transmission is essential for high performance.

The results of the numerical simulations and analytical calculations is outlined in the section 3 of supplementary data. Initial analytical predictions, shown in figure S1, established a photonic bandgap in the 3–5 μm wavelength range, with a periodicity between 0.85 μm and 1.74 μm for oxide holes in the SiGe membrane. This periodicity was further refined through phonon bandgap simulations, as shown in figure S2, revealing low-loss terahertz (THz) phonon transmission and suppression of GHz phonons, a critical feature for maintaining signal integrity. Figure S3 presents transmission loss (TL) data, confirming GHz phonon

suppression, which enhances overall device performance. Furthermore, figure S4 illustrates the efficient light confinement within the Ge core, showing minimal scattering and optimal mode propagation at 3.4375 μm, while figures S6–S8 provide detailed analysis of the dispersion, group delay, and propagation constant across the MWIR range. These figures highlight how the waveguide maintains uniform transmission, minimizing signal distortion. The combination of photonic and phononic bandgaps, as seen in figure S5, ensures high transmission efficiency across the MWIR spectrum, making this design highly suitable for high-sensitivity sensing applications.

The findings of this study not only contribute to the advancement of Terahertz photonic applications but also highlight the potential of Ge/SiGe slot waveguides in overcoming the limitations of existing technologies. The lower transmission loss and wider bandwidth of the proposed waveguide offer new possibilities for the development of high-performance photonic devices. Further research and experimentation in this direction could lead to significant advancements in Terahertz photonics, with implications for various fields such as communications, sensing, and imaging. The concept of mirror symmetry within the Phoxonic crystal (PxC) structure plays a pivotal role in reducing phonon dispersion. By ensuring that the structural elements of the waveguide are arranged symmetrically, one can effectively control the propagation of phonons. This symmetry helps to localize specific phonon frequencies, thereby minimizing energy losses associated with phonon scattering and improving overall waveguide performance. Finally, the Phoxonic waveguide shows promise for real-world applications, particularly in telecommunications and medicine. In telecommunications, its high transmission efficiency could lead to improved optical communication systems with enhanced data rates and reliability. In medical applications, the waveguide's sensitivity in the mid-wave infrared range can facilitate advanced imaging techniques, contributing to non-invasive diagnostic methods. However, challenges such as fabrication complexity, integration with existing systems, scalability, and regulatory hurdles must be addressed to ensure successful implementation and widespread adoption.

7. Conclusion

The novel mathematical model presented in this study anticipates significant advancements in the design of on-chip optical waveguides for the Mid-Wave Infrared (MWIR) spectrum. The model's key findings and implications include exceptional transmission rates of up to 99.8% throughout the MWIR range (3–5 μm). This performance is achieved through an innovative mirror-symmetric architecture that effectively suppresses losses caused by photon-phonon interactions, defining the Phoxonic crystal waveguide. The Phoxonic crystal waveguide represents a significant advancement in enhancing transmission properties by simultaneously controlling photon and phonon transmission. This breakthrough architecture, enabled by the model, contributes to the exceptional transmission rates achieved in the MWIR range. The numerical simulations using the open source python-based platform, Qutip is used to validate the model's effectiveness in terms of suppression of high-frequency phonons. Hence being able to accurately enhance the waveguide transmission uniformly over desired spectrum. The development of MWIR waveguides with such high transmission rates holds promise for communication, defense, medicine, and technology applications.

Data availability statement

The data cannot be made publicly available upon publication because no suitable repository exists for hosting data in this field of study. The data that support the findings of this study are available upon reasonable request from the authors.

Declarations

We, the authors, declare that this work is original, has not been published elsewhere, and involves no conflicts of interest. All authors have approved the final manuscript for submission.

Ethical approval

Hereby, I Anurag Sharma consciously assure that for the manuscript 'Mathematical Model for Enhancing Midwave Infrared Transmission Using Phoxonic Crystals 'the following is fulfilled: 1) This material is the authors' own original work, which has not been previously published elsewhere. 2) The paper is not currently being considered for publication elsewhere.

Competing interests

I declare that they have no known competing financial interests or personal relationships that could have appeared to influence the work reported in this paper.

Authors' contributions

'All authors contributed to the study conception and design. Material preparation, data collection and analysis were performed by Anurag Sharma, Dr Jyoti Kedia and Dr Neena Gupta. The first draft of the manuscript was written by Anurag Sharma and all authors commented on previous versions of the manuscript. All authors read and approved the final manuscript.'

Funding

'Here by, all authors declare that no funds, grants, or other support were received during the preparation of this manuscript.'

ORCID iDs

Anurag Sharma https://orcid.org/0000-0003-1737-7966

References

[1] Guo R, Gao H, Cheng Z and Liu T 2021 Advances on mid-infrared germanium integrated photonics *Zhongguo Jiguang/Chinese Journal of Lasers* **48** 1901002
[2] Qu Z *et al* 2018 Waveguide integrated graphene mid-infrared photodetector *Proc. SPIE Silicon Photonics XIII* 10537 *(San Francisco, California, United States, 27 JANUARY - 1 FEBRUARY 2018)* in
[3] Cheng Z 2019 Mid-infrared germanium photonics *international Photonics and OptoElectronics Meeting* paper OTh3C.2. (*(OFDA, OEDI, ISST, PE, LST, TSA) OSA Technical Digest (Optica Publishing Group) (, Wuhan China, 11–14 November)* 2019
[4] Carletti L *et al* 2015 Mid-infrared nonlinear optics in SiGe waveguides *EEE Summer Topicals Meeting Series (SUM) (Nassau, Bahamas)* (IEEE) pp 59–60
[5] Hu T *et al* 2017 Silicon photonic platforms for mid-infrared applications [Invited] *Photonics Research* **5** 417–30
[6] Sharma A, Kedia J and Gupta N 2020 Nanostructured material engineering for ultra-low loss MWIR thermal sensors-a short review *Mater. Today Proc.* **28** 1709–13
[7] Ao L and Ramiere A 2023 Phoxonic bandgap modulation in optomechanical crystals with shifting hole *J. Phys. D: Appl. Phys.* **56** 065102
[8] Lei L, Yu T, Liu W, Wang T and Liao Q 2022 Dirac cones with zero refractive indices in phoxonic crystals *Opt. Express* **30** 308–17
[9] Zhao S *et al* 2023 Topological phoxonic crystals for simultaneously controlling electromagnetic and elastic waves *Physics Letters, section A: General, Atomic and Solid State Physics* **475** 128851
[10] Wang Z *et al* 2018 Acousto-optic interactions for terahertz waves using phoxonic quasicrystals *J. Phys. D: Appl. Phys.* **51** 105110
[11] Aly A H, Shaban S M and Mehaney A 2021 High-performance phoxonic cavity designs for enhanced acousto-optical interaction *Appl. Opt.* **60** 3224–323
[12] Gupta N, Kedia J and Sharma A 2021 Emerging nanostructured infrared absorbers enabling cost-effective image sensing: a review *Opt. Eng.* **60** 090901
[13] Osman A *et al* 2018 Suspended low-loss germanium waveguides for the longwave infrared *Opt. Lett.* **43** 5997–6000
[14] Liu X *et al* 2022 MEMS enabled suspended silicon waveguide platform for long-wave infrared modulation applications *Int. J. Optomechatronics* **16** 42–57
[15] Sánchez-Postigo A *et al* 2021 Suspended germanium waveguides with subwavelength-grating metamaterial cladding for the mid-infrared band *Opt. Express* **29** 16867–78
[16] Butsch A, Conti C, Biancalana F and Russell P S J 2012 Optomechanical self-channeling of light in a suspended planar dual-nanoweb waveguide *Phys. Rev. Lett.* **108** 093903
[17] Sharma A, Kedia J and Gupta N 2023 Multispectral transmission through phoxonic crystal slot-waveguide at midwave infrared frequencies *Opt. Eng.* **62** 047101
[18] Johansson J R, Nation P D and Nori F 2012 QuTiP: an open-source python framework for the dynamics of open quantum systems *Comput. Phys. Commun.* **183** 1760–72
[19] Ho D *et al* 2011 FDTD simulation of inverse 3D face-centered cubic photonic crystal cavities *IEEE J. Quantum Electron.* **47** 1480–92
[20] Eggleton B J, Poulton C G, Rakich P T, Steel M J and Bahl G 2019 Brillouin integrated photonics *Nat. Photonics* **13** 664–77
[21] Wiederhecker G S, Dainese P and Alegre T P M 2019 Brillouin optomechanics in nanophotonic structures Brillouin optomechanics in nanophotonic structures *APL Photonics* **07** 1101
[22] Wolff C, Smith M J A, Stiller B and Poulton C G 2021 Brillouin scattering—theory and experiment: tutorial *J. Opt. Soc. Am.* B **38** 1243–69
[23] Forzani L, Mendez C G, Urteaga R and Huespe A E 2021 Design and optimization of an opto-acoustic sensor based on porous silicon phoxonic crystals *Sens Actuators A Phys.* **331** 112915
[24] Lucklum R, Zubtsov M and Oseev A 2013 Phoxonic crystals-a new platform for chemical and biochemical sensors *Anal Bioanal Chem* **405** 6497–509

[25] Li H, Liu W, Yu T, Wang T and Liao Q 2020 Simultaneous unidirectional reciprocal filters of electromagnetic and elastic waves based on the modal symmetry of phoxonic crystal waveguides and cavity *Physics Letters, section A: General, Atomic and Solid State Physics* **384** 126499
[26] Shu Y *et al* 2020 Design of phoxonic virtual waveguides for both electromagnetic and elastic waves based on the self-collimation effect: an application to enhance acousto-optic interaction *Opt. Express* **28** 24813–19
[27] Psarobas I E *et al* 2010 Enhanced acousto-optic interactions in a one-dimensional phoxonic cavity *Phys. Rev. B Condens. Matter Mater. Phys.* **82** 174303
[28] Qiu W, Rakich P T, Shin H and Dong H 2013 Stimulated brillouin scattering in nanoscale silicon step-index waveguides : a general framework of selection rules and calculating SBS gain *OPTICS EXPRESS* **21** 25 31402
[29] Lodahl P *et al* 2017 Chiral quantum optics, *Nature* **541** 473–80
[30] Zoubi H and Hammerer K 2017 Quantum nonlinear optics in optomechanical nanoscale waveguides *Phys. Rev. Lett.* **119** 123602
[31] Talebzadeh R, Beiranvand R and Moayed S H 2023 Design and simulation of an all-optical Fredkin gate based on silicon slab-waveguide in a 2D photonic crystal *Opt. Quantum Electron.* **55** 241
[32] Fang K, Matheny M H, Luan X and Painter O 2016 Optical transduction and routing of microwave phonons in cavity-optomechanical circuits *Nat. Photonics* **10** 489–96
[33] Yu S, Piao X and Park N 2019 Chirality in non-hermitian photonics *Curr. Opt. Photon.* **3** 275–84
[34] Johnson S G *et al* 2002 Perturbation theory for Maxwell's equations with shifting material boundaries *Phys Rev E Stat Phys Plasmas Fluids Relat Interdiscip Topics* **65** 066611
[35] Wang X *et al* 2022 Non-Hermitian high-quality-factor topological photonic crystal cavity *Phys Rev A (Coll Park)* **105** 023531